

RESEARCH ARTICLE

Thermodynamic Simulation of Carbonate Cements-Water-Carbon Dioxide Equilibrium in Sandstone for Prediction of Precipitation/Dissolution of Carbonate Cements

Yiping Duan^{1,2}*, Mingshi Feng²*, Xinyan Zhong¹, Ruishu Shang¹, Lihong Huang^{1,3}*

1 Department of Chemical and Pharmaceutical Engineering, Chengdu University of Technology, Chengdu, China, **2** State Key Laboratory of Oil and Gas Reservoir Geology and Exploitation, Chengdu University of Technology, Chengdu, China, **3** Richard G. Lugar Center for Renewable Energy, Indiana University-Purdue University, Indianapolis, IN, United States

* These authors contributed equally to this work.

* fengmingshi09@cdut.cn (MF); huanglihong06@cdut.cn, lihhuang@iupui.edu (LH)



OPEN ACCESS

Citation: Duan Y, Feng M, Zhong X, Shang R, Huang L (2016) Thermodynamic Simulation of Carbonate Cements-Water-Carbon Dioxide Equilibrium in Sandstone for Prediction of Precipitation/Dissolution of Carbonate Cements. *PLoS ONE* 11(12): e0167035. doi:10.1371/journal.pone.0167035

Editor: Varenyam Achal, East China Normal University, CHINA

Received: April 25, 2016

Accepted: November 8, 2016

Published: December 1, 2016

Copyright: © 2016 Duan et al. This is an open access article distributed under the terms of the [Creative Commons Attribution License](https://creativecommons.org/licenses/by/4.0/), which permits unrestricted use, distribution, and reproduction in any medium, provided the original author and source are credited.

Data Availability Statement: All relevant data are within the paper.

Funding: This work was financially supported by the Open Fund (PLC201205) of State Key Laboratory of Oil and Gas Reservoir Geology and Exploitation (Chengdu University of Technology), the National Natural Science Foundation of China (21276031), and by the Department of Science and Technology of Sichuan Province (2015HH0013). The funders had no role in study design, data

Abstract

Carbonate cements, such as calcite, dolomite, ferrocalcite and ankerite, play important roles in the formation of pores in sandstones: precipitation of carbonate cements modifies pores and inhibits compaction, while dissolution creates secondary pores. This work proposed a precipitation-dissolution model for carbonate cements-CO₂-H₂O system by means of ion equilibrium concentration ($[M^{2+}]$, M = Ca, Mg, Fe or Mn) with different factors, such as temperature, depth, pH, P_{CO_2} , variable rock composition and overpressure. Precipitation-dissolution reaction routes were also analyzed by minimization of the total Gibbs free energy (ΔG). $\Delta[M^{2+}]$, the variation of $[Ca^{2+}]$, $[Fe^{2+}]$, $[Mg^{2+}]$ or $[Mn^{2+}]$ for every 100 m of burial depths, is used to predict precipitation or dissolution. The calculation results indicate that the increasing temperature results in decrease of equilibrium constant of reactions, while the increasing pressure results in a relatively smaller increase of equilibrium constant; As a result, with increasing burial depth, which brings about increase of both temperature and pressure, carbonate cements dissolve firstly and produces the maximal dissolved amounts, and then precipitation happens with further increasing depth; For example, calcite is dissolving from 0.0 km to 3.0 km with a maximal value of $[Ca^{2+}]$ at depth of 0.8 km, and then precipitates with depth deeper than 3.0 km. Meanwhile, with an increasing CO₂ mole fraction in the gaseous phase from 0.1% to 10.0% in carbonate systems, the aqueous concentration of metal ions increases, e.g., dissolved amount of CaFe_{0.7}Mg_{0.3}(CO₃)₂ increases and reaches maximum of 1.78 mmol·L⁻¹ and 8.26 mmol·L⁻¹ at burial depth of 0.7 km with CO₂ mole fraction of 0.1% and 10.0%, respectively. For the influence of overpressure in the calcite system, with overpressure ranging from 36 MPa to 83 MPa, pH reaches a minimum of 6.8 at overpressure of 51 MPa; meanwhile, $\Delta[Ca^{2+}]$ increases slightly from -2.24 mmol·L⁻¹ to -2.17 mmol·L⁻¹ and remains negative, indicating it is also a precipitation process at burial depth of 3.9 km where overpressure generated. The method used in this study can be applied in assessing burial precipitation-dissolution processes and predicting possible pores in reservoirs with carbonate cement-water-carbon dioxide.

collection and analysis, decision to publish, or preparation of the manuscript.

Competing Interests: The authors have declared that no competing interests exist.

Introduction

For petroleum reservoirs, about one-third are consisted of carbonate rocks, which include calcite and binary or ternary carbonates with Mg, Fe or Mn, e.g., dolomite ($\text{CaMg}(\text{CO}_3)_2$), ferro-calcite ($\text{Ca}_{0.9}\text{Fe}_{0.1}\text{CO}_3$) and ankerite ($\text{CaFe}_{0.5}\text{Mn}_{0.5}(\text{CO}_3)_2$) [1,2]. Within these carbonate reservoirs, secondary pores are considered as the main storage space, and was formed via water-rock interaction at different burial depths during diagenesis [3–5]. Besides, for diagenesis of source rocks, organic acid and CO_2 can be released into sandstone pores and may lead to the dissolution of carbonate and formation of secondary pores [6]. And in recent years, to cut CO_2 emission into the atmosphere from fossil-fuel power stations, geological sequestration or underground storage of CO_2 in depleted oil and gas reservoirs has been investigated [7–10]; as a result, the initial physic-chemical equilibrium between the fluid and carbonate cements can be disturbed and dissolution or precipitation of carbonate cements may occur accordingly [11]. Prediction of precipitation-dissolution of carbonates can be also applied in microbially induced calcium-carbonate precipitation(MICP), in which nucleation sites and enzyme of urease and carbonic anhydrase play important roles for this biochemical process, while factors of the calcium concentration (Ca^{2+}), the concentration of dissolved inorganic carbon and the pH are critical for formation of carbonates [12–14].

To predict precipitation/dissolution of carbonate cements at different burial depth with CO_2 , systems of calcite or dolomite-water-carbon dioxide under acidic condition were typically analyzed via ion equilibrium as well as minimization of Gibbs free energy (ΔG) and equilibrium constant [15,16]. For example, for the carbonate cements, $\Delta[\text{Ca}^{2+}]$, the variation of $[\text{Ca}^{2+}]$ for every 100 m of burial depths, was analyzed in calcite and dolomite system [3,16]: if $\Delta[\text{Ca}^{2+}]$ is positive, dissolution of carbonate happens; otherwise, precipitation takes place.

During diagenesis of carbonate cements, the main factors concerned include temperature, pressure, pH, P_{CO_2} , variable rock composition, hydrologic regime, fluid composition, organic acid anion, etc. [17,18]. Among these factors, temperatures play an important role: For the rock- H_2O - CO_2 system at different temperatures of 55°C, 70°C and 100°C, the corrosion of feldspars, silica and clay minerals intensifies with increasing temperature [19]. For CO_2 in these systems, aqueous concentration of metal ions increased with increasing P_{CO_2} in carbonate cements [20,21].

Within carbonates, there are binary or ternary minerals of carbonate cements with Mg, Fe or Mn, which are common in reservoir of sandstones [1]; these carbonates are important in formation of secondary pores via precipitation/dissolution within systems of carbonates- H_2O - CO_2 in reservoirs. However, study on thermodynamic equilibrium model and ionic concentrations in these binary or ternary minerals has been few reported. Meanwhile, effect of variable rock composition in ankerite, e.g., $\text{CaFe}_x\text{Mg}_{1-x}(\text{CO}_3)_2$ ($0 \leq x \leq 1$) during diagenesis is also a concern in thermodynamic calculation because of unavailability of thermodynamic data.

Overpressure, another factor that influences thermodynamic equilibrium as well as dissolution/precipitation, can be found at reservoirs where fluid pressure exceeds the hydrostatic pressure [22]. The reason of overpressure can be attributed to disequilibrium compaction, diagenesis and hydrocarbon generation, which involves in total organic carbon and hydrogen index [22]. Overpressure generated in source rock can be estimated via parameters of hydrogen index and total organic carbon [23], and can also be used to analyze dissolution/precipitation of carbonate cements in source rocks.

In this work, the authors 1) calculated ΔG and equilibrium constant of reactions in carbonate cements-water-carbon dioxide systems via chemical thermodynamic principles, 2) used $\Delta[M^{2+}]$ ($M = \text{Ca}^{2+}$, Fe^{2+} , Mg^{2+} , or Mn^{2+}) to predict precipitation/dissolution in systems of

carbonate cements-water-carbon dioxide, and 3) discussed the parameters, e.g., temperature, pressure, depth, pH, P_{CO_2} and overpressure, that influence the chemical equilibrium and precipitation/dissolution. This model can be applied in carbonate cements with binary or ternary minerals in ferrocalcite and ankerite ($CaFe_xMg_{1-x}(CO_3)_2$, $0 \leq x \leq 1$) systems for prediction of precipitation/dissolution in sandstone reservoirs.

Method

The thermodynamic equilibrium model

Temperature and pressure are important parameters in diagenesis at different burial depth; a temperature gradient of 0.03 K/m and a pressure gradient of 1.0 MPa/100m with a surface pressure of 10^5 Pa are given in this work.

The main reactions and equilibrium constant expressions in water-carbon dioxide system and carbonate cement dissociations are listed in Table 1.

In the current work, the concentrations of carbonate were used because in dilute solutions, concentrations of carbonates are approximately equal to the activities, and the calculation process can be simplified [16].

The direction of those reactions can be analyzed by the Gibbs free energy (ΔG), while ΔG at different temperatures and pressures can be calculated via Eq 1 [24]:

$$\Delta_r G^0 = \Delta_r H_{T_{ref}}^0 - T\Delta_r S_{T_{ref}}^0 + \int_{T_{ref}}^T \Delta_r C_p dT - \int_{T_{ref}}^T \frac{\Delta_r C_p}{T} dT + \int_{P_{ref}}^P \Delta_r V dP \quad (1)$$

where:

$\Delta_r H_{T_{ref}}^0$ standard molar enthalpy of the reaction at 298.15 K and 10^5 Pa

$\Delta_r S_{T_{ref}}^0$ standard molar entropy of the reaction at 298.15 K and 10^5 Pa

Table 1. The equilibrium reactions and equilibrium constant expressions in carbonate-H₂O-CO₂ system

Equilibrium reactions in carbonate-H ₂ O-CO ₂	Equilibrium constant expressions ^a
$CO_2(g) + H_2O \rightleftharpoons H_2CO_3$	$K_1 = \frac{[H_2CO_3]}{P_{CO_2}}$
$H_2CO_3 \rightleftharpoons H^+ + HCO_3^-$	$K_2 = \frac{[H^+][HCO_3^-]}{[H_2CO_3]}$
$HCO_3^- \rightleftharpoons H^+ + CO_3^{2-}$	$K_3 = \frac{[H^+][CO_3^{2-}]}{[HCO_3^-]}$
$H_2O \rightleftharpoons H^+ + OH^-$	$K_4 = [H^+][OH^-]$
$CaCO_3 \rightleftharpoons Ca^{2+} + CO_3^{2-}$	$K_5 = [Ca^{2+}][CO_3^{2-}]$
$CaMg(CO_3)_2 \rightleftharpoons Ca^{2+} + Mg^{2+} + 2CO_3^{2-}$	$K_6 = [Ca^{2+}][Mg^{2+}][CO_3^{2-}]^2$
$Ca_{0.9}Fe_{0.1}CO_3 \rightleftharpoons 0.9Ca^{2+} + 0.1Fe^{2+} + CO_3^{2-}$	$K_7 = [Ca^{2+}]^{0.9}[Fe^{2+}]^{0.1}[CO_3^{2-}]$
$CaFe_{0.5}Mg_{0.5}(CO_3)_2 \rightleftharpoons Ca^{2+} + 0.5Mg^{2+} + 0.5Fe^{2+} + 2CO_3^{2-}$	$K_8 = [Ca^{2+}][Mg^{2+}]^{0.5}[Fe^{2+}]^{0.5}[CO_3^{2-}]^2$
$CaFe(CO_3)_2 \rightleftharpoons Ca^{2+} + Fe^{2+} + 2CO_3^{2-}$	$K_9 = [Ca^{2+}][Fe^{2+}][CO_3^{2-}]^2$
$MgCO_3 \rightleftharpoons Mg^{2+} + CO_3^{2-}$	$K_{10} = [Mg^{2+}][CO_3^{2-}]$
$FeCO_3 \rightleftharpoons Fe^{2+} + CO_3^{2-}$	$K_{11} = [Fe^{2+}][CO_3^{2-}]$
$CaFe_{0.5}Mn_{0.5}(CO_3)_2 \rightleftharpoons Ca^{2+} + 0.5Fe^{2+} + 0.5Mn^{2+} + 2CO_3^{2-}$	$K_{12} = [Ca^{2+}][Mn^{2+}]^{0.5}[Fe^{2+}]^{0.5}[CO_3^{2-}]^2$
$MnCO_3 \rightleftharpoons Mn^{2+} + CO_3^{2-}$	$K_{13} = [Mn^{2+}][CO_3^{2-}]$

^a [X] in mmol·L⁻¹ represents the concentration of species X, and K is the thermodynamic equilibrium constant

doi:10.1371/journal.pone.0167035.t001

C_p heat capacity at constant pressure, $C_p/J \cdot K^{-1} \cdot mol^{-1} = a + b(T/K) + c(T/K)^{-2}$, in which a , b and c are the coefficients in the heat capacity polynomial.

V molar volume of solid phase and liquid phase

T_{ref} the temperature at 298.15K

P_{ref} the pressure at 10^5 Pa

$$\int_{10^5}^P \Delta_r V dP = [(\sum_B \nu_B V_S^0)_{production} - (\sum_B \nu_B V_S^0)_{reactant}](P - 10^5) + \nu_B \int_{10^5}^P \Delta_r V_m dP \quad (2)$$

where:

V_s the molar volume of solid phase, including ion and solid mineral phase.

V_m the molar volume of liquid phase, which was calculated by the Soave-Redlich-Kwong (SRK) equation, which is capable to predict molar volume of CO_2 and H_2O , as listed in Eq 3 [25,26].

$$P = \frac{RT}{V - b} - \frac{a\alpha(T)}{V(V + b)} \quad (3)$$

where

$$a = 0.42748 \frac{R^2 T_c^2}{P_c} \quad (4)$$

$$b = 0.08664 \frac{RT_c}{P_c} \quad (5)$$

$$\alpha(T) = (1 + (0.485 + 1.574\omega - 0.176\omega^2)(1 - \sqrt{T_r}))^2 \quad (6)$$

The critical temperature (T_c), critical pressure (P_c) and acentric factor (ω) were applied in SRK equation and are listed in Table 2 [27].

Based on ΔG , the equilibrium constant of reactions (K) can be calculated via Eq 7:

$$\Delta G = \Delta G_0 + RT \ln K \quad (7)$$

in which ΔG_0 is the standard Gibbs free energy of the reaction at 298.15K and 10^5 Pa, T is the absolute temperature in Kelvin, and R is the gas constant ($8.314 J \cdot K^{-1} \cdot mol^{-1}$).

In the system of calcite-water-carbon dioxide, the charge balance equations or electroneutrality are calculated by the positive and negative ions as followed [28]:

$$[H^+] + 2[Ca^{2+}] = 2[CO_3^{2-}] + [HCO_3^-] + [OH^-] \quad (8)$$

For the systems of the dolomite or ankerite, Eq 8 can be revised as Eq 9.

$$[H^+] + 2[Ca^{2+}] + 2[Fe^{2+}] + 2[Mg^{2+}] \text{ (or } [Mn^{2+}]) = 2[CO_3^{2-}] + [HCO_3^-] + [OH^-] \quad (9)$$

According to the equilibrium expressions of H_2O-CO_2 (Table 1), electroneutrality equation

Table 2. The critical values of carbon dioxide and water

	$T_c(K)$	$P_c(bar)$	ω
$CO_2(g)$	304.2	73.8	0.224
H_2O	647.1	220.6	0.345

doi:10.1371/journal.pone.0167035.t002

(Eq 9) with different carbon dioxide pressure (P_{CO_2}) and the equilibrium constants (K or K') of carbonate, the quartic equation related to $[H^+]$ can be obtained via Eqs 10 and 11, as followed:

$$\left(\frac{2K}{K_1 \cdot K_2 \cdot K_3 \cdot (P_{CO_2})}\right)[H^+]^4 + [H^+]^3 - (K_1 \cdot K_2 \cdot (P_{CO_2}) + K_4)[H^+] - 2(P_{CO_2}) \cdot K_1 \cdot K_2 \cdot K_3 = 0 \tag{10}$$

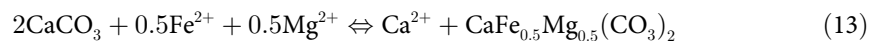
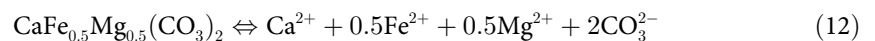
$$\left(\frac{4\sqrt{K'}}{K_1 \cdot K_2 \cdot K_3 \cdot (P_{CO_2})}\right)[H^+]^4 + [H^+]^3 - (K_1 \cdot K_2 \cdot (P_{CO_2}) + K_4)[H^+] - 2(P_{CO_2}) \cdot K_1 \cdot K_2 \cdot K_3 = 0 \tag{11}$$

Eq 10 can be applied in the systems of $MCO_3-CO_2-H_2O$ ($M = Ca, Fe, Mg$ or Mn) and $Ca_{0.9}Fe_{0.1}CO_3-CO_2-H_2O$, while Eq 11 can be applied to in the system of dolomite or ankerite.

Based on $[H^+]$, the concentration of other species, such as $[Ca^{2+}]$, $[HCO_3^-]$ and $[OH^-]$, can be calculated according to equilibrium expressions and equilibrium constant of reaction, while $\Delta[Ca^{2+}]$, the variation of $[Ca^{2+}]$ equilibrium concentration for every 100 m of burial depths, can be calculated to predict precipitation or dissolution occurring in carbonate cement system.

Thermodynamic data of ferrocalcite and ankerite

The standard Gibbs free energy of formation ($\Delta_f G_0$) of minerals can be found from databases or literatures [29–31], while neither equilibrium constant nor $\Delta_f G_0$ for ferrocalcite ($Ca_{0.9}Fe_{0.1}CO_3$) and ankerite ($CaFe_{0.5}Mg_{0.5}(CO_3)_2$) can be found to calculate the equilibrium concentration. However, a linear correlation exists between Gibbs free energies of formation of calcite-like carbonate and the corresponding aqueous divalent cations, and can be used to estimate the basic thermodynamic value of ferrocalcite ($Ca_{0.9}Fe_{0.1}CO_3$) [32]. Meanwhile, the equation of ankerite dissociation (Eq 12) can be deduced by combining calcite dissociation and Eq 13, and the corresponding equilibrium constant of ankerite dissociation ($CaFe_{0.5}Mg_{0.5}(CO_3)_2$), K_8 , is shown in Eq 14, while K^* is the equilibrium constant of Eq 13:



$$K_8 = \frac{[Ca^{2+}][Fe^{2+}]^{0.5}[Mg^{2+}]^{0.5}[CO_3^{2-}]^2}{K_1^2} \tag{14}$$

$$K^* = \frac{[Ca^{2+}]}{[Fe^{2+}]^{0.5}[Mg^{2+}]^{0.5}} = \frac{[Ca^{2+}][CO_3^{2-}]}{[Fe^{2+}]^{0.5}[Mg^{2+}]^{0.5}[CO_3^{2-}]} \tag{15}$$

The thermodynamic data used in this work are shown in Table 3.

Because of the instability in solution, carbonic acid can be treated as $CO_2(g)$ dissolved in water as $CO_2(aq)$ [35,36]. When $\frac{T}{T_c} \leq 0.98$, Bhirud Equation in Eq 16 can be applied to calculate its molar volume; when $\frac{T}{T_c} > 0.98$, molar volume is considered as a constant because the

Table 3. The thermodynamic data of carbonate minerals. Data from [33] and [34] are marked as^{-a} and^{-b}.

Species	$\Delta_f H$ (kJ/mol)	S (J/mol/K)	V (cm ³ /mol)	$C_p / J \cdot K^{-1} \cdot mol^{-1} = a + b(T/K) + c(T/K)^{-2}$		
				a	b	c
Calcite ^{-a}	-1207.88	92.50	36.89	140.9	0.005029	-950700
Dolomite ^{-a}	-2325.76	156.10	64.29	358.9	-0.00495	0
Magnesite ^{-a}	-1110.93	65.50	28.03	186.4	-0.003772	0
Siderite ^{-a}	-762.22	93.30	29.43	168.4	0	0
Rhodochrosite ^{-a}	-892.28	98.00	31.07	169.5	0	0
CaFe(CO ₃) ₂ ^{-a}	-1970.62	188.46	66.06	341.0	0.001161	0
Ca _{0.1} Fe _{0.9} (CO ₃) ₂	-1178.19	92.678	36.16	87.1	0.052325	2093000
CO ₂ (g) ^{-a}	-393.51	213.7	0	87.8	-0.002644	706400
H ₂ O(aq) ^{-b}	-285.8	70	18.07	30.5	0.0103	0
H ₂ CO ₃ ^{-b}	-699.648	187.443	-	0.000	0.70291	0
Ca ²⁺ ^{-a}	-543.3	-56.50	-18.06	0	0.069	0
Mg ²⁺ ^{-a}	-465.96	-138.10	-21.55	0	0.0462	0
Fe ²⁺ ^{-a}	-90.42	-107.11	-22.20	0	0	0
Mn ²⁺ ^{-a}	-220.39	-73.57	-17.1	0	0.04184	0
H ⁺ ^{-a}	0	0	0	0	0	0
OH ⁻ ^{-a}	-230.02	-10.71	-4.18	0	0	0
HCO ₃ ⁻ ^{-b}	-691.992	91.211	24.6	0.000	-0.12468	0
CO ₃ ²⁻ ^{-a}	-675.23	-50.00	-5.02	0	0	0

doi:10.1371/journal.pone.0167035.t003

influence of temperature and pressure on molar volume is slight in the liquid phase [37].

$$\ln\left(\frac{P_c V}{RT}\right) = \ln u^0 + \ln u^1 = \ln u \tag{16}$$

Where: u^0 and u^1 are dimensionless and are a function of $T_r = \frac{T}{T_c}$.

$$\begin{aligned} \ln u^0 = & -0.40062 - 8.0006T_r + 49.3780T_r^2 - 170.6616T_r^3 + 287.6989T_r^4 \\ & - 232.5608T_r^5 + 73.03299T_r^6 \end{aligned} \tag{17}$$

$$\begin{aligned} \ln u^1 = & 13.4412 - 135.7437T_r + 533.38T_r^2 - 1091.453T_r^3 + 1231.43T_r^4 \\ & - 728.227T_r^5 + 176.737T_r^6 \end{aligned} \tag{18}$$

To verify the estimated thermodynamic data obtained by the current thermodynamic calculation method (TCM), the Helgeson-Kirkham-Flowers (HKF) equation was used for comparison [38]. The equilibrium constants of bicarbonate (K_3) and water dissociation (K_4) were selected and calculated by methods of TCM and HKF, respectively, and the results and relative differences are listed in Table 4; the results indicate that TCM is an effective

Table 4. Comparison of equilibrium constants calculated by thermodynamic calculation method (TCM) and HKF equation in system of CO₂-H₂O

P(Pa)	T(K)	K ₃			K ₄		
		TCM	HKF ^{-a}	Δ	TCM	HKF ^{-a}	Δ
1.0	298.15	4.57×10 ⁻¹¹	4.69×10 ⁻¹¹	-2.56%	1.03×10 ⁻¹⁴	1.00×10 ⁻¹⁴	2.91%
1000.0	373.15	2.38×10 ⁻¹⁰	2.42×10 ⁻¹⁰	-1.65%	5.48×10 ⁻¹³	5.38×10 ⁻¹³	1.86%

^{-a} [3]

doi:10.1371/journal.pone.0167035.t004

Table 5. The overpressure, $\Delta_r G$ and equilibrium constant in $\text{CaFe}(\text{CO}_3)_2\text{-H}_2\text{O-CO}_2$ system

Overpressure(MPa)	$\Delta_r V^0(P-P^0)(\text{m}^3 \cdot \text{Pa}^{-1} \cdot \text{mol}^{-1})$	$\Delta_r G(\text{kJ} \cdot \text{mol}^{-1})$	lgK
36	-4177.32	176.44	-22.20
51	-5922.72	174.70	-21.98
65	-7551.76	173.07	-21.78
78	-9064.44	171.56	-21.59
83	-9646.24	170.97	-21.51

in which P^0 is the pressure at 10^5 Pa

doi:10.1371/journal.pone.0167035.t005

way to calculate the equilibrium constant, as compared with HKF equation, while less parameters are needed for TCM.

The effect of variable composition in ankerite system and overpressure in carbonate systems

The thermodynamic method was used to analyze the influence of variable rock composition in the ankerite system ($\text{CaFe}_x\text{Mg}_{1-x}(\text{CO}_3)_2$, $0 \leq x \leq 1$), in which $\text{CaFe}_{0.2}\text{Mg}_{0.8}(\text{CO}_3)_2$, $\text{CaFe}_{0.3}\text{Mg}_{0.7}(\text{CO}_3)_2$, $\text{CaFe}_{0.5}\text{Mg}_{0.5}(\text{CO}_3)_2$, $\text{CaFe}_{0.7}\text{Mg}_{0.3}(\text{CO}_3)_2$ and $\text{CaFe}(\text{CO}_3)_2$ are selected and named as ank2, ank3, ank5, ank7 and ank10, respectively.

Overpressure is defined as fluid pressure exceeding the hydrostatic pressure, and is always found in the burial depth from 3.2 km and 3.9 km; for example, overpressure was reported with variation up to 83 MPa at 3.9 km in simulation experiments [23]. Based on the values of overpressure from 36 MPa to 83 MPa, a $\text{CaFe}(\text{CO}_3)_2$ system with 800 mg/g of hydrogen index at a burial depth of 3.9 km was selected, and data of $\Delta_r G$ and equilibrium constant were calculated, as listed in Table 5.

The overall methodology is shown in Fig 1: the minimization of ΔG and equilibrium constant of reactions were calculated in carbonate cements-water-carbon dioxide systems via

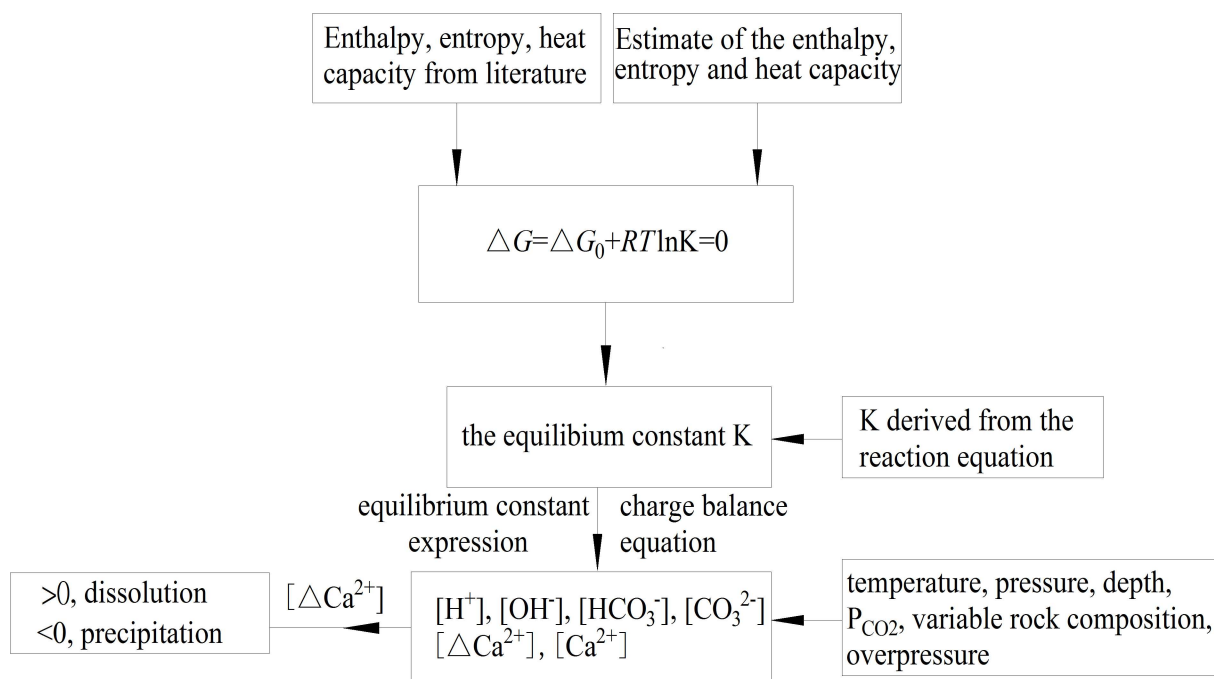


Fig 1. Flow diagram of the calculation method.

doi:10.1371/journal.pone.0167035.g001

chemical thermodynamic parameters, and the $\Delta[M^{2+}]$ ($M = Ca^{2+}, Fe^{2+}, Mg^{2+},$ or Mn^{2+}) were analyzed to predict precipitation/dissolution with variable parameters, e.g., temperature, pressure, depth, pH, P_{CO_2} , variable rock composition and overpressure.

Results and Discussion

Chemical equilibrium constant of reactions in carbonate-water-carbon dioxide system

The equilibrium constants calculated from ΔG of reaction can be used to calculate equilibrium constant and to analyze equilibrium concentration of ions, such as $[Ca^{2+}]$, $[Mg^{2+}]$, $[Fe^{2+}]$ or $[Mn^{2+}]$. The influence of 1) temperature, 2) pressure and 3) burial depth on equilibrium constant of calcite- H_2O - CO_2 was firstly analyzed.

As shown in Table 6, when the temperature increases from 301.15 K to 478.15 K, lgK decreases from -8.53 to -9.69; meanwhile, when the pressure increases from 15 to 70 MPa at 301.15 K, lgK increase slightly from -8.53 to -7.82. The result indicates that temperature has a higher impact on lgK on an opposite direction, as compared with pressure. As a result, when the burial depth increases from 1.5 km to 6.0 km, the temperature increases from 343.15 K to 478.15K and pressure increases from 15 MPa to 60 MPa; meanwhile, lgK decreases from -8.69 to -9.39.

Based on the aforementioned method, the equilibrium constants of carbonates- H_2O - CO_2 at different depths were then calculated, as shown in Fig 2. The results indicate that lgK are negative at different burial depth, while the ΔG are positive ($\Delta G = -RT \ln K$), indicating that those processes cannot take place automatically.

For the water-carbon dioxide system in Fig 2A, the equilibrium constant of carbon dioxide dissolving in water and forming carbonic acid, lgK_1 , ranges from -1.12 to -1.97 and reaches the minimum of -1.97 at depth of 4.0 km. LgK_2 (the equilibrium constant of carbonic acid dissociation) reaches the maximum of -6.23 at about 1.5 km, and then decreases continuously with further increasing depth. The equilibrium constant of secondary dissociation of carbonic acid, lgK_3 , ranges from -10.31 to -8.60 at the depth from 0.0 km to 7.0 km, which is about three orders of magnitude lower than K_2 . Furthermore, the equilibrium constant of water dissociation, lgK_4 , is increasing from -14.00 to -10.10 with increasing burial depth.

For the equilibrium constant of carbonate cement dissociation in Fig 2B, calcite (K_5) and magnesite (K_{10}) show a similar trend of decreasing with burial depth increased. Meanwhile, the equilibrium constant of ferrocalcite dissociation (K_7) locates between those of calcite (K_5) and siderite (K_{11}); in the mean time, the equilibrium constants of dolomite (K_6), $CaFe_{0.5}Mg_{0.5}(CO_3)_2$ (K_8), $CaFe(CO_3)_2$ (K_9) and $CaFe_{0.5}Mn_{0.5}(CO_3)_2$ (K_{12}) in Fig 2C are several orders of magnitude lower than those of other carbonate cements in Fig 2B. Through the

Table 6. ΔG and equilibrium constants (K) with different temperatures, pressures and burial depths in calcite- H_2O - CO_2

Depth(km)	Temperature(K)	Pressure(MPa)	ΔG (J/mol)	lgK
-	301.15	15	49166.56	-8.53
-	478.15	15	88688.97	-9.69
-	301.15	50	46288.02	-8.03
-	301.15	70	45088.62	-7.82
0	298.15	0.1	48681.85	-8.53
1.5	343.15	15	57103.05	-8.69
4.0	418.15	40	72544.71	-9.06
6.0	478.15	60	85970.32	-9.39

doi:10.1371/journal.pone.0167035.t006

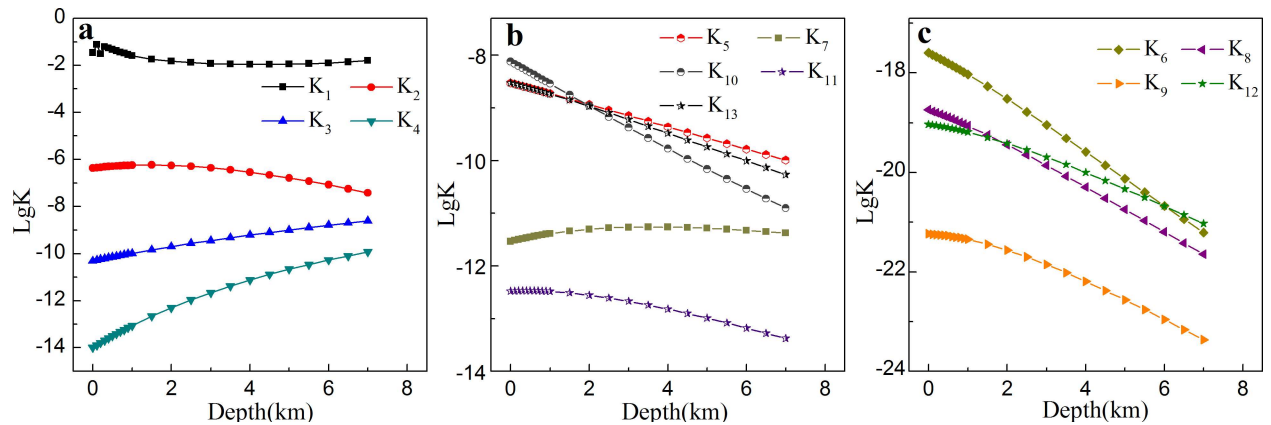


Fig 2. The equilibrium constants (K_1 - K_{13}) at different burial depth in carbonate-water-carbon dioxide system. (a): the equilibrium constants in water-carbon dioxide systems; (b-c): the equilibrium constants in carbonate cements-water-carbon dioxide.

doi:10.1371/journal.pone.0167035.g002

equilibrium constants, the concentrations of dissolved species in aqueous solution were then calculated.

Calculation of $\Delta[M^{2+}]$ for prediction of precipitation/dissolution of carbonate cements with different CO_2 mole fraction

The data of 1) $\Delta[Ca^{2+}]$ in calcite, dolomite, ferrocalcite and ankerite, 2) $\Delta[Fe^{2+}]$ in siderite, 3) $\Delta[Mg^{2+}]$ in magnesite and 4) $\Delta[Mn^{2+}]$ in rhodochrosite were analyzed; in these cases, $\Delta[M^{2+}]$ is defined as the variation of equilibrium $[M^{2+}]$ for every 100 m of burial depths, and can indicate the dissolution or precipitation during diagenesis.

As shown in Fig 3A, with the CO_2 mole fraction at 0.1%, the systems of calcite, dolomite, magnesite and rhodochrosite are shown a trend of dissolving because $\Delta[M^{2+}]$ are positive at depth from 0.0 km to 3.2 km, 2.7 km, 1.8 km and 2.0 km, respectively, indicating the secondary pores may form during this dissolution process; and in this dissolution process, the systems of calcite, dolomite, magnesite and rhodochrosite produce maximal concentrations of 1.37, 0.52, 1.35 and 0.58 $mmol \cdot L^{-1}$ at depth of 0.8 km, 0.7 km, 0.5 km and 0.5 km. As to systems of calcite and dolomite, the amount of dolomite dissolved was smaller than that of calcite at different depth, thus the dolomitization of limestone may decrease the porosity [39,40]. With further increasing depth deeper than 3.2 km, 2.7 km, 1.8 km and 2.0 km in cements of calcite, dolomite, magnesite and rhodochrosite, respectively, $\Delta[M^{2+}]$ turns to negative, suggesting that precipitation occurs in these systems.

On the other hand, carbon dioxide partial pressure has effect on these systems of carbonate cements-water-carbon dioxide, as shown in Fig 3: with increasing CO_2 mole fraction, the systems of calcite, dolomite, magnesite and rhodochrosite still show a similar trend of dissolving firstly and then precipitating with the increasing depth, while the maximal values are also obtained at the same depths. Nevertheless, the maxima of dissolving amount in systems of calcite, dolomite, magnesite and rhodochrosite were obtained near depth of 0.5–0.8 km, and increase by about four times with the partial pressure of carbon dioxide increasing from 0.1% to 10.0%, indicating that increasing partial pressure of CO_2 results in the instability or dissolution of these carbonate cements, thus promoting the formation of secondary pore [41].

The relationship between $\Delta[M^{2+}]$ and depth in cements of $CaFe_{0.5}Mg_{0.5}(CO_3)_2$, $Ca_{0.9}Fe_{0.1}(CO_3)_2$, $CaFe(CO_3)_2$, $FeCO_3$ and $CaFe_{0.5}Mn_{0.5}(CO_3)_2$ at different CO_2 mole fraction are shown in Fig 3D–3F. These five carbonate cements show a similar trend of dissolution

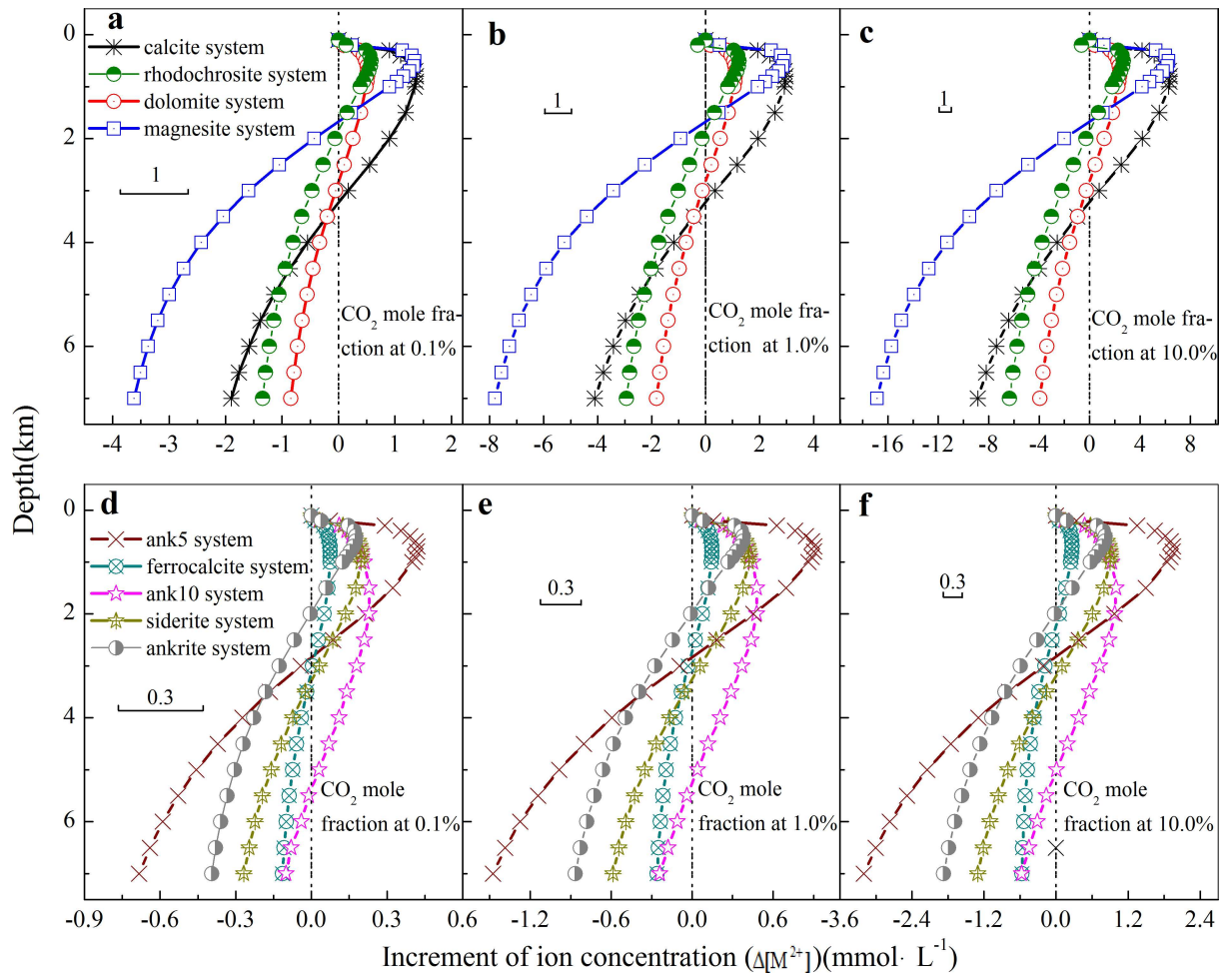


Fig 3. The increment of ion concentration, $\Delta[M^{2+}]$, as a function of depth in carbonate cement systems with 1) $\Delta[Ca^{2+}]$ in calcite, dolomite, ferrocalsite and ankerite, 2) $\Delta[Fe^{2+}]$ in siderite, 3) $\Delta[Mg^{2+}]$ in magnesite and 4) $\Delta[Mn^{2+}]$ in rhodochrosite, in which $\Delta[M^{2+}]$ is defined as the variation of $[M^{2+}]$ for every 100 m of burial depths.

doi:10.1371/journal.pone.0167035.g003

firstly followed by precipitation. For example, in the $CaFe_{0.5}Mg_{0.5}(CO_3)_2$ system, dissociation happens within 0.0–3.0 km and precipitation occurs with depth deeper than 3.0 km, which is similar to the results reported by [1]: in Wilcox (Eocene) sandstones, ankerite ($CaFe_{0.5}Mg_{0.5}(CO_3)_2$) precipitates at depths deeper than 3.2 km. The slight difference in depth can be attributed to geological factors, such as the burial history, organic acid anions and chemical compaction. In Fig 3D–3F, with the carbon dioxide mole fraction increasing from 0.1% to 10.0%, the maximal amounts of dissolved cements increase and obtained near depth of 0.7–0.9 km. For example, the maximal dissolved siderite ($FeCO_3$) at depth of 0.7 km increases from $0.21 \text{ mmol}\cdot\text{L}^{-1}$ to $0.86 \text{ mmol}\cdot\text{L}^{-1}$ with CO_2 mole fraction increasing from 0.1% to 10.0%.

The relationship between carbonate species concentration and P_{CO_2} in ankerite ($CaFe_{0.5}Mg_{0.5}(CO_3)_2$) system at depth of 2.5 km

For carbonate cements- H_2O - CO_2 systems with different cements and CO_2 mole fraction, carbonate species, e.g., HCO_3^- and CO_3^{2-} , play an important role in dissolution/precipitation of

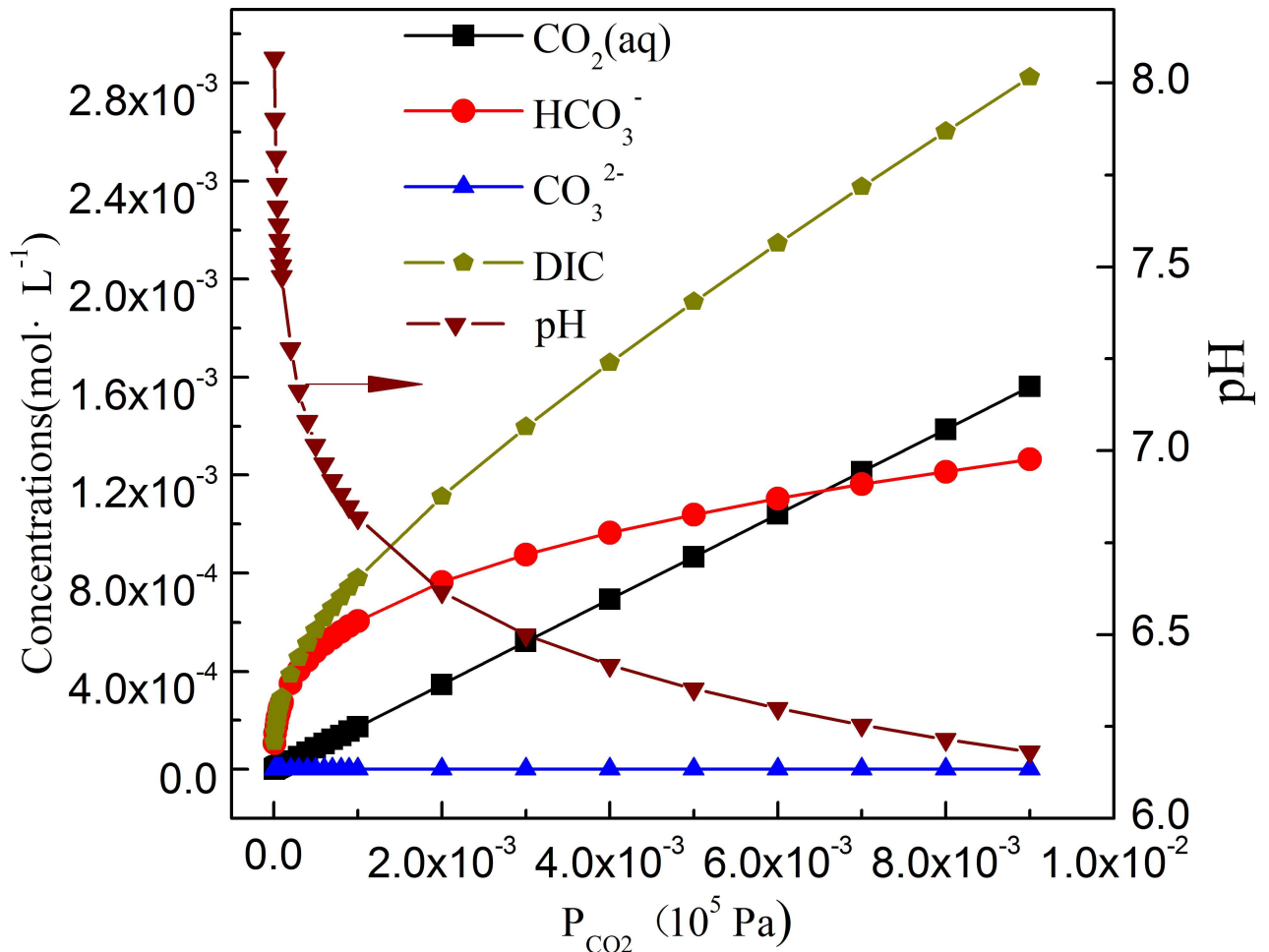


Fig 4. Distribution of carbonate species in $\text{CaFe}_{0.5}\text{Mg}_{0.5}(\text{CO}_3)_2$ system as a function of P_{CO_2} at 373.15 K and 25 MPa. (DIC, total dissolved inorganic carbon, $\text{DIC} = [\text{CO}_2(\text{aq})] + [\text{HCO}_3^-] + [\text{CO}_3^{2-}]$)

doi:10.1371/journal.pone.0167035.g004

cements. System of $\text{CaFe}_{0.5}\text{Mg}_{0.5}(\text{CO}_3)_2$ was then selected as a model to analyze effect of CO_2 mole fraction on variation of carbonate species (total dissolved inorganic carbon, $\text{DIC} = [\text{CO}_2(\text{aq})] + [\text{HCO}_3^-] + [\text{CO}_3^{2-}]$) at burial depth of 2.5 km with 373.15 K and 25 MPa. As shown in Fig 4, pH decrease from 7.6 to 6.2 with P_{CO_2} increasing from 0 MPa to 1.0×10^{-3} MPa, while the total amount of DIC, $[\text{CO}_2(\text{aq})]$, $[\text{HCO}_3^-]$ increase continuously. $[\text{CO}_3^{2-}]$ varies at a range of 1.28×10^{-3} – 1.95×10^{-4} $\text{mmol} \cdot \text{L}^{-1}$, and is about three orders of magnitude smaller than that of $[\text{HCO}_3^-]$.

The pH at different depth in carbonate cements- H_2O - CO_2 systems

The relationship between pH at different CO_2 mole fraction and depth in carbonate cement systems was also analyzed and is shown in Fig 5. For the calcite system in Fig 5A, the pH decreases from 7.9 to 5.8 with increasing burial depth from 0.0 km to 7.0 km at CO_2 mole fraction 0.1%, and this variation can be attributed to the dissolution of primary minerals [42]. It is worth to note that as the depth increases from 0.0 km to 1.0 km, pH decreases sharply from 7.9 to 6.4. For the effect of CO_2 mole fraction, pH decreases from 6.0 to 5.3 and to 4.6 with CO_2 mole fraction increasing from 0.1% to 1.0% and to 10.0%, respectively, at depth of 4.0 km.

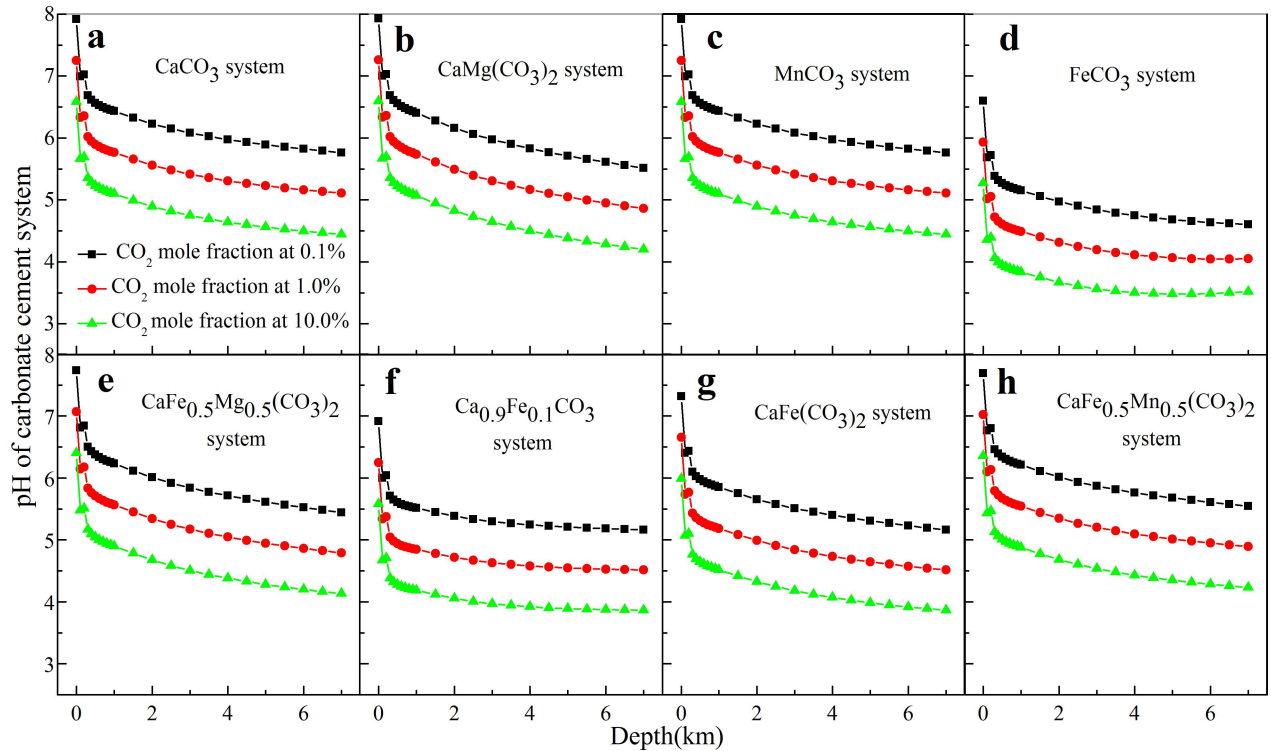


Fig 5. pH of carbonate cements-H₂O-CO₂ system with different burial depth and CO₂ mole fraction.

doi:10.1371/journal.pone.0167035.g005

Other carbonate cements in Fig 5B–5H show a similar trend of decreasing pH with increasing CO₂ mole fraction. Among these cements, the siderite-water-carbon dioxide system produces the lowest pH of 3.5 at depth of 4.0 km (CO₂ mole fraction 10.0%), which can be attributed to hydrolysis of ferrous ion [43].

The main dissolved species generated during the dissolution process in carbonate cements

To find the main species generated during the dissolution/precipitation process, the relationship between calcium and bicarbonate ion at different depth was analyzed. In Fig 6A of the calcite system, [HCO₃⁻] is increasing from 1.21 mmol·L⁻¹ to a maximum of 4.32 mmol·L⁻¹ as depth ranging from 0.0 km to 0.8 km with CO₂ mole fraction of 0.1%; with depth deeper than 0.8 km, [HCO₃⁻] is decreasing to 0.59 mmol·L⁻¹ at 7.0 km. Other carbonate cements also show a similar trend.

For the effect of CO₂, with increasing CO₂ mole fraction from 0.1% to 10.0%, [HCO₃⁻] increases remarkably at the same depth, as shown in Fig 6. For example, [HCO₃⁻] in the calcite system increases from 4.32 mmol·L⁻¹ to 20.07 mmol·L⁻¹ with CO₂ mole fraction increasing from 0.1% to 10.0% at depth of 0.8 km.

The relationship between [Ca²⁺] and [HCO₃⁻] was studied as well, and a linear relationship was found, as shown in Fig 7: in the calcite system, [HCO₃⁻] increases from 1.21 mmol·L⁻¹ to 4.32 mmol·L⁻¹ at 0.1% of CO₂ mole fraction when depth increasing from 0.0 km to 0.8 km, and [Ca²⁺] increases linearly from 0.61 mmol·L⁻¹ to 2.16 mmol·L⁻¹ (Fig 7A). With increasing CO₂ mole fraction from 0.1% to 10.0%, there is still a linear relationship in other carbonate cements, as shown in Fig 7.

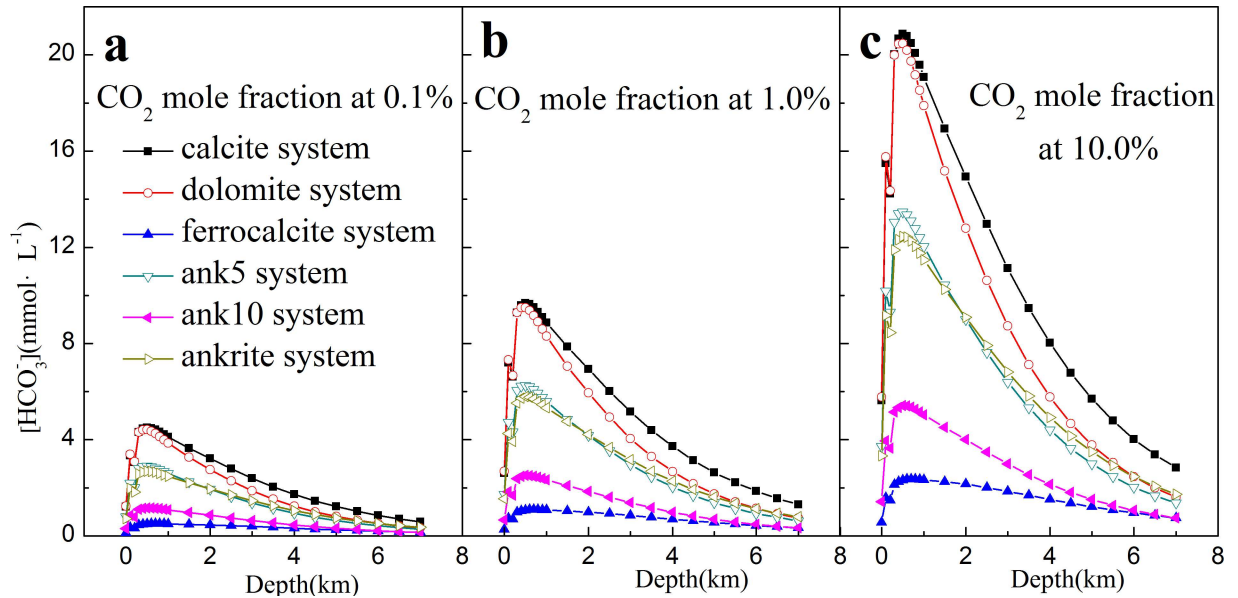


Fig 6. $[HCO_3^-]$ as a function of depth with different CO_2 mole fraction in carbonate cements- CO_2 - H_2O systems.

doi:10.1371/journal.pone.0167035.g006

The influence of variable rock composition in ankerite- H_2O - CO_2 system

Ankerite consists of variable compositions, and the influence of variable composition on precipitation/dissolution was analyzed. As shown in Fig 8A, $\Delta[Ca^{2+}]$ indicates that ankerite ($CaFe_xMg_{1-x}(CO_3)_2$, $0 \leq x \leq 1$) system dissolves at depth smaller than 3.5 km with a maximal dissolved amount at depth of 0.8 km, but precipitates with depth deeper than 3.5 km. With the increasing Fe content (from ank2 to ank7), the amount of dissolved or precipitated carbonates

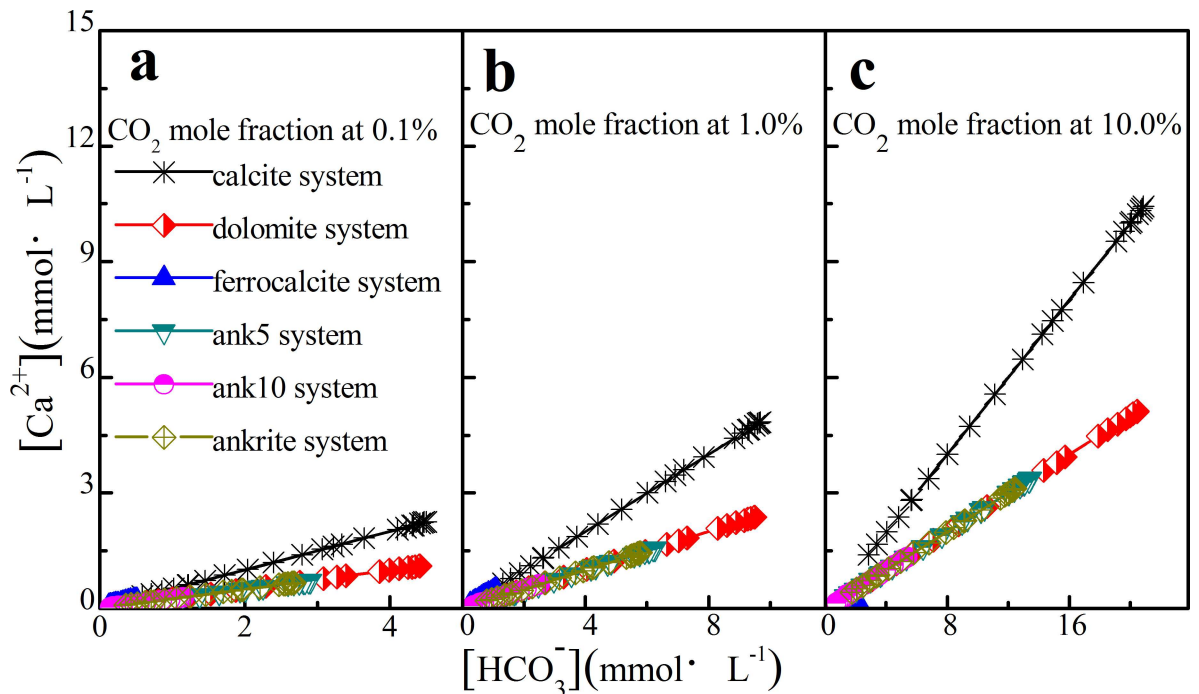


Fig 7. The linear relationship between $[Ca^{2+}]$ and $[HCO_3^-]$.

doi:10.1371/journal.pone.0167035.g007

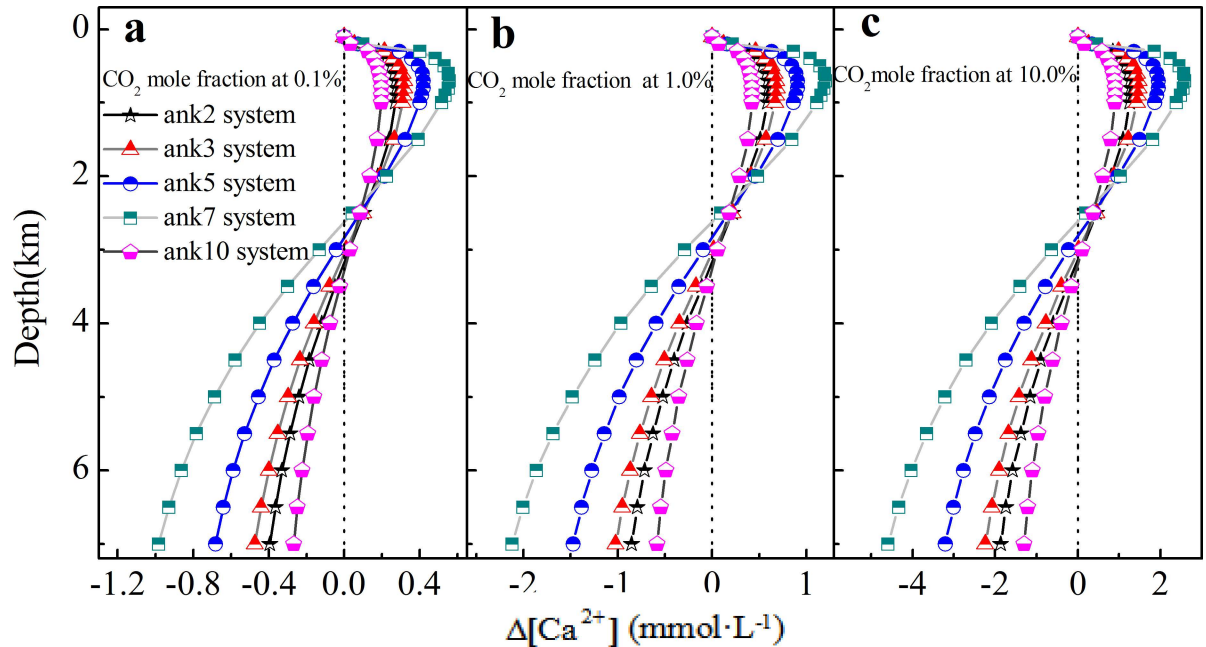


Fig 8. The variation of calcium ion at different burial depth in ankerite system with variable compositions.

doi:10.1371/journal.pone.0167035.g008

is also increased. Meanwhile, $\text{CaFe}(\text{CO}_3)_2$ (ank10) is an exception: the amount of precipitation or dissolution is the lowest among these ankerite cements. The reason can be attributed to that the end-member of $\text{CaFe}(\text{CO}_3)_2$ mainly exists as a two-phase mineral with both calcite and siderite [44]. On the effect of CO_2 , $\Delta[\text{Ca}^{2+}]$ increases by about four times with CO_2 mole fraction increasing from 0.1% to 10.0%, which is shown in Fig 8, indicating that the amount of dissolved carbonate cements also increases with increasing CO_2 mole fraction.

The relationship between pH and concentration of $[\text{Ca}^{2+}]$ in ankerite- H_2O - CO_2 system was also studied. As shown in Fig 9A of ank2 system, with the decrement of pH, $[\text{Ca}^{2+}]$ reaches the maximum of $0.80 \text{ mmol}\cdot\text{L}^{-1}$ at CO_2 mole fraction of 0.1%, indicating dissolution may happen; then the $[\text{Ca}^{2+}]$ drops with pH further decreasing, indicating there can be precipitation and formation of carbonate cement. With increasing CO_2 mole fraction, the maxima of $[\text{Ca}^{2+}]$

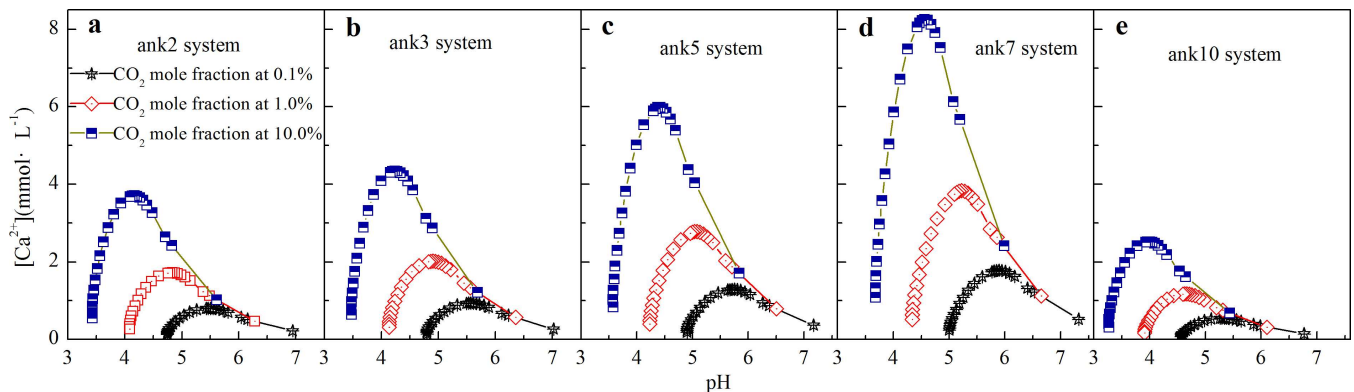


Fig 9. The relationship between pH and $[\text{Ca}^{2+}]$ in ankerite- H_2O - CO_2 system.

doi:10.1371/journal.pone.0167035.g009

increase and emerge at lower pHs, e.g., 0.80 mmol·L⁻¹ at pH = 5.5 for 0.1% of CO₂, 1.72 mmol·L⁻¹ at pH = 4.8 for 1.0% of CO₂, and 3.70 mmol·L⁻¹ at pH = 4.2 for 10.0% of CO₂ in system of ank2. With increment of Fe content in ankerite (CaFe_xMg_{1-x}(CO₃)₂, 0 ≤ x ≤ 1) system, as shown in Fig 9A–9D), the maximum of [Ca²⁺] also increases as well. The ank10 (CaFe(CO₃)₂) is an exception: as shown in Fig 9E, [Ca²⁺] varies from 0.3 mmol·L⁻¹ to 2.5 mmol·L⁻¹ in CaFe(CO₃)₂ at CO₂ mole fraction of 10.0%, which is the lowest in ankerite system, and can also be attributed to that the end-member of CaFe(CO₃)₂ does not exist as one-phase mineral [44].

The influence of overpressure on carbonate cements-H₂O-CO₂

The pressure variation during diagenesis can be applied to estimate the overpressure and to calculate the equilibrium constant. Effect of overpressure on carbonates systems was studied at depth of 3.9 km with 800 mg/g of hydrogen index where overpressure generated. As shown in Fig 10A, with the increasing overpressure, the equilibrium constants of 1) formation of carbonic acid (K₁), 2) formation of bicarbonate (K₂) and 3) water dissociation (K₄) decrease. Meanwhile, the equilibrium constants of dissociation of carbonate cements (K₅-K₁₃) increase with increasing overpressure in Fig 10B and 10C. For example, over ferrocalcite (Ca_{0.9}Fe_{0.1}CO₃), the equilibrium constant (K₇) ranges from 7.8 × 10⁻¹² to 2.2 × 10⁻¹¹ with overpressure increasing from 36 MPa to 83 MPa. The equilibrium constants of dolomite (K₆), CaFe_{0.5}Mg_{0.5}(CO₃)₂ (K₈) and CaFe(CO₃)₂ (K₉) are several orders of magnitude lower than those of other carbonate cements.

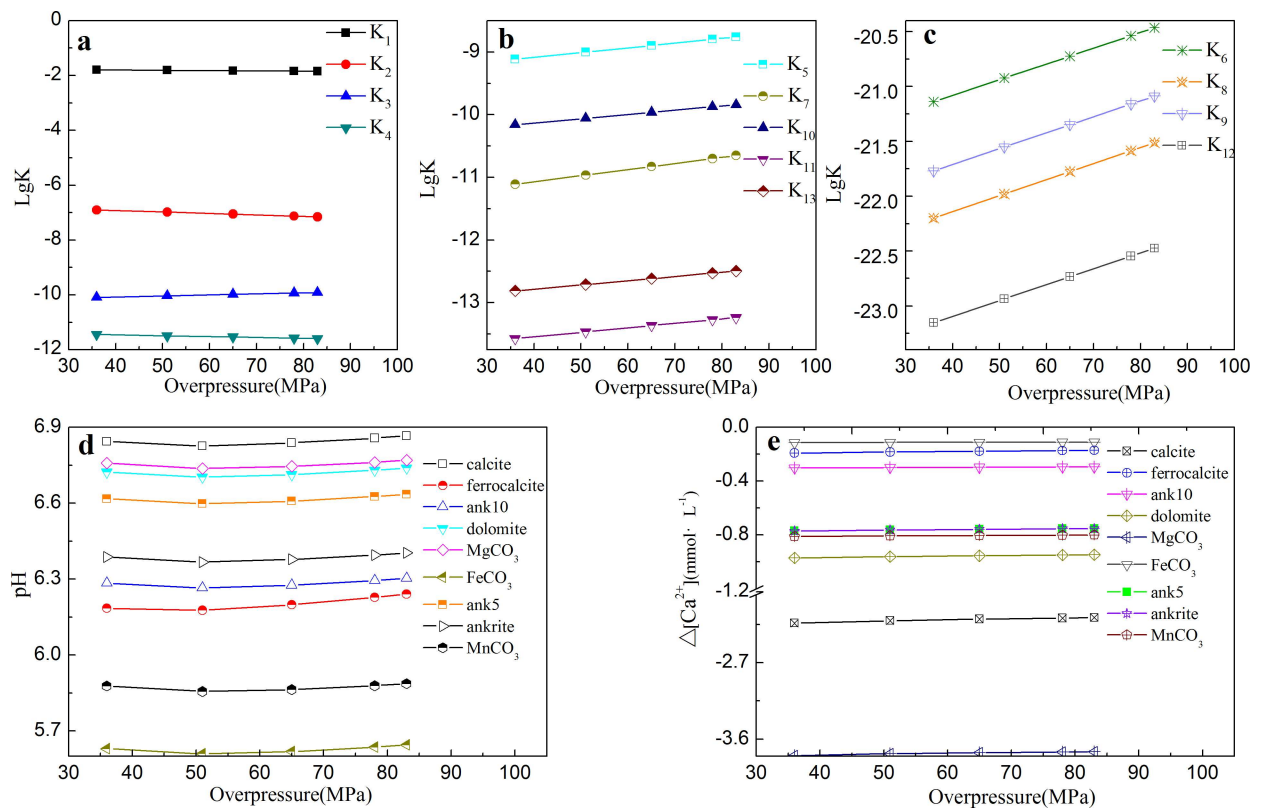


Fig 10. The equilibrium constant and overpressure at depth of 3.9 km with 800 mg/g of hydrogen index, (d) The relationship between overpressure and pH with CO₂ mole fraction 0.1% at a burial depth of 3.9 km with 800 mg/g of hydrogen index, and (e) Δ[Ca²⁺] at different overpressures with CO₂ mole fraction of 0.1%.

doi:10.1371/journal.pone.0167035.g010

The relationship between overpressure and pH was also analyzed, as shown in Fig 10D. The overpressure ranging from 36 MPa to 83 MPa at CO₂ mole fraction of 0.1% leads to a minimal pHs of 6.8, 6.2, 6.3 and 6.4 at 51 MPa in the systems of calcite, ferrocalcite (Ca_{0.9}Fe_{0.1}CO₃), ank10(CaFe(CO₃)₂) and ankerite(CaFe_{0.5}Mn_{0.5}(CO₃)₂), respectively. Meanwhile, system of siderite (FeCO₃) produces the lowest pH at this range of overpressure.

Effect of overpressure on Δ[Ca²⁺] was studied as well. As shown in Fig 10E, in the calcite system, with increasing overpressure from 36 MPa to 83 MPa, Δ[Ca²⁺] increases slightly from -2.24 mmol·L⁻¹ to -2.17 mmol·L⁻¹ and remains negative, indicating it is still a precipitation process at depth of 3.9 km where overpressure generated. Other carbonate cements also show a similar trend of precipitation at depth of 3.9 km where overpressure generated, and the magnesite system produces the lowest Δ[Ca²⁺] from -3.79 mmol·L⁻¹ to -3.75 mmol·L⁻¹. This result is helpful to predict the accumulated space or reservoir formed in sandstone and source rock during diagenesis.

Conclusions

The minimization of ΔG and equilibrium constant of reactions in carbonate cements-water-carbon dioxide systems were calculated via chemical thermodynamic principles. Δ[M²⁺], calculated from equilibrium concentration, was applied to predict the precipitation/dissolution process.

The results indicate that with increasing burial depth, carbonate cements with binary or ternary minerals in ferrocalcite and ankerite (CaFe_xMg_{1-x}(CO₃)₂, 0 ≤ x ≤ 1) dissolve firstly and produce maximal dissolved amounts, while precipitation happens later. For example, calcite is dissolving from 0.0 km to 3.0 km with the maximal value of [Ca²⁺] obtained at depth of 0.8 km, and then precipitates with deeper depth than 3.0 km.

On effect of CO₂ mole fraction, with the increasing CO₂ mole fraction from 0.1% to 10.0% in carbonate system, the aqueous concentrations of metal species show a similar trend of increase firstly and then decrease. For example, dissolved amount of CaFe_{0.7}Mg_{0.3}(CO₃)₂ increases and reaches a maximum of 1.78 mmol·L⁻¹ at a burial depth of 0.7 km with CO₂ mole fraction at 0.1%, while 8.26 mmol·L⁻¹ is obtained at the same depth of 0.7 km with 10.0% of CO₂.

For the influence of overpressure generated during diagenesis, with the overpressure ranging from 36MPa to 83 MPa in calcite system, Δ[Ca²⁺] increases slightly from -2.24 mmol·L⁻¹ to -2.17 mmol·L⁻¹, indicating it is also a precipitation process at burial depth of 3.9 km where overpressure generated.

Author Contributions

Conceptualization: LH MF YD.

Data curation: YD MF LH.

Formal analysis: YD MF LH.

Funding acquisition: LH MF.

Investigation: YD MF LH.

Methodology: LH YD MF.

Project administration: LH MF.

Resources: MF YD LH.

Software: YD LH RS.

Supervision: LH MF.

Validation: YD MF XZ.

Writing – original draft: YD LH MF.

Writing – review & editing: LH MF YD.

References

1. Boles J R. Active ankerite cementation in the subsurface eocene of southwest texas. *Contrib Mineral Petr.* 1978; 68: 13–22.
2. Zenger D H, Dunham J B, Ethington L R. Concepts and models of dolomitization. 1980. pp. 320.
3. Yu B S, Dong H L, Ruan Z. Mechanism for calcite dissolution and its contribution to development of reservoir porosity and permeability in the Kela 2 gas field, Tarim Basin, China. *Sci China Ser D.* 2008; 51: 567–578.
4. Rossi C, Marfil R, Ramseyer K, Permanyer A. Facies-related diagenesis and multiphase siderate cementation and dissolution in the reservoir sandstone of the Khatatba formation, Egypt's western desert. *J Sediment Res.* 2001; 71: 459–472.
5. Jin Z J, Zhu D Y, Hu W X, Zhang X F, Zhang J T, Song Y C. Mesogenetic dissolution of the middle Ordovician limestone in the Tahe oilfield of Tarim basin, NW China. *Mar Petrol Geol.* 2009; 26: 753–763.
6. Bloch S, Lander R H, Bonnell L. Anomalously high porosity and permeability in deeply buried sandstone reservoirs: Origin and predictability. *Aapg Bull.* 2002; 82: 301–328.
7. Sung R T, Li M H, Dong J J, Lin Tien-Shun A, Hsu S K, Wang C Y, et al. Numerical assessment of CO₂ geological sequestration in sloping and layered heterogeneous formations: A case study from Taiwan. *Int J Greenh Gas Con.* 2014; 20: 168–179.
8. Ketzner J M, Iglesias R, Einloft S, Dullius J, Ligabue R, Lima V D. Water–rock–CO₂ interactions in saline aquifers aimed for carbon dioxide storage: Experimental and numerical modeling studies of the Rio Bonito Formation (Permian), southern Brazil. *Appl Geochem.* 2009; 24: 760–767.
9. Zhao J, Lu W, Zhang F J, Lu C, Du J J, Zhu R Y, et al. Evaluation of CO₂ solubility-trapping and mineral-trapping in microbial-mediated CO₂–brine–sandstone interaction. *Mar Pollut Bull.* 2014; 85: 78–85. doi: [10.1016/j.marpolbul.2014.06.019](https://doi.org/10.1016/j.marpolbul.2014.06.019) PMID: [25015018](https://pubmed.ncbi.nlm.nih.gov/25015018/)
10. Yao L L, Shi J Y, Miao X L. Mixed Wastewater Coupled with CO₂ for Microalgae Culturing and Nutrient Removal. *PLoS one.* 2015; 10: e0139117. doi: [10.1371/journal.pone.0139117](https://doi.org/10.1371/journal.pone.0139117) PMID: [26418261](https://pubmed.ncbi.nlm.nih.gov/26418261/)
11. Fischer S, Liebscher A, Wandrey M. CO₂–brine–rock interaction—First results of long-term exposure experiments at in situ P–T conditions of the Ketzin CO₂ reservoir. *Chem Erde—Geochem.* 2010; 70: 155–164.
12. Achal V, Pan X. Characterization of Urease and Carbonic Anhydrase Producing Bacteria and Their Role in Calcite Precipitation. *Curr Microbiol.* 2011; 62: 894–902. doi: [10.1007/s00284-010-9801-4](https://doi.org/10.1007/s00284-010-9801-4) PMID: [21046391](https://pubmed.ncbi.nlm.nih.gov/21046391/)
13. Achal V, Mukherjee A, Kumari D, Zhang Q. Biomineralization for sustainable construction—A review of processes and applications. *Earth-Science Reviews.* 2015; 148: 1–17.
14. Hammes F, Boon N, Clement G, de Villiers J, Siciliano S D, Verstraete W. Molecular, biochemical and ecological characterisation of a bio-catalytic calcification reactor. *Appl Microbiol Biot.* 2003; 62: 191–201.
15. Huang S J, Xiao L P, Yang J J, Zhang W Z, Huang Y M, Liu G H. Experimental Simulation of Dolomite Dissolution Under Burial Diagenesis Conditions and Thermodynamic Interpretation. *Chin J Geochem.* 2000; 19: 58–64.
16. Ruan Z, Yu B S, Wang L D, Pan Y L, Tan G H. Prediction of buried calcite dissolution in the Ordovician carbonate reservoir of the Tahe Oilfield, NW china: Evidence from formation water. *Chem Erde—Geochem.* 2013; 73: 469–479.
17. Tempel R N, Harrison W J. Simulation of burial diagenesis in the Eocene Wilcox Group of the Gulf of Mexico basin. *Appl Geochem.* 2000; 15: 1071–1083.
18. Haase C, Dethlefsen F, Ebert M, Dahmke A. Uncertainty in geochemical modelling of CO₂ and calcite dissolution in NaCl solutions due to different modelling codes and thermodynamic databases. *Appl Geochem.* 2013; 33: 306–317.

19. Wang T Y, Wang H Y, Zhang F J, Xu T F. Simulation of CO₂-water-rock interactions on geologic CO₂ sequestration under geological conditions of China. *Mar Pollut Bull.* 2013; 76: 307–314. doi: [10.1016/j.marpolbul.2013.08.014](https://doi.org/10.1016/j.marpolbul.2013.08.014) PMID: [24035426](https://pubmed.ncbi.nlm.nih.gov/24035426/)
20. Wunsch A, Navarre-Sitchler A K, Moore J, Ricko A, McCray J E. Metal release from dolomites at high partial-pressures of CO₂. *Appl Geochem.* 2013; 38: 33–47.
21. Lin C Y, Musta B, Abdullah M H. Geochemical processes, evidence and thermodynamic behavior of dissolved and precipitated carbonate minerals in a modern seawater/freshwater mixing zone of a small tropical island. *Appl Geochem.* 2013; 29: 13–31.
22. Al-Najrani F. Analysis of overpressure generating mechanisms in different tectonic settings. UMI dissertation publishing: The University of Texas at San Antonio. 2010.
23. Guo X W, He S, Liu K Y, Zheng L J. Quantitative estimation of overpressure caused by oil generation in petroliferous basins. *Org Geochem.* 2011; 42: 1343–1350.
24. Belonoshko A, Saxena A K. A molecular dynamics study of the pressure-volume-temperature properties of super-critical fluids: I. H₂O. *Geochim Cosmochim Ac.* 1991; 55: 381–387.
25. Li H, Yan J. Impacts of equations of state (EOS) and impurities on the volume calculation of CO₂ mixtures in the applications of CO₂ capture and storage (CCS) processes. *Appl Energ.* 2009; 86: 2760–2770.
26. Delavar H., Haghtalab A. Prediction of hydrate formation conditions using G^E-EOS and UNIQUAC models for pure and mixed-gas systems. *Fluid Phase Equilib.* 2014; 369: 1–12.
27. Camy S, Pic J S, Badens E, Condoret J S. Fluid phase equilibria of the reacting mixture in the dimethyl carbonate synthesis from supercritical CO₂. *J Supercrit Fluid.* 2003; 25: 19–32.
28. Georg K, Dreybrodt W. Calcite dissolution kinetics in the system CaCO₃-H₂O-CO₂ at high undersaturation. *Geochim Cosmochim Ac.* 2007; 71: 1398–1410.
29. Helgeson H C, Delany J M, Nesbitt W H, Bird D K. Summary and critique the thermodynamic properties of rock-forming minerals. *Am J Sci.* 1978; 278-A: 1–229.
30. Shock E L, Helgeson H C. Calculation of the thermodynamic and transport properties of aqueous species at high pressures and temperatures: Correlation algorithms for ionic species and equation of state predictions to 5 kb and 1000°C. *Geochim Cosmochim Ac.* 1988; 52: 2009–2036.
31. Holland T J B, Powell R. An internally consistent thermodynamic data set for phases of petrological interest. *J Metamorph Geol.* 1998; 16: 309–343.
32. Sverjensky D A. Prediction of Gibbs free energies of calcite type carbonates and the equilibrium distribution of trace elements between carbonates and aqueous solution. *Geochim Cosmochim Ac.* 1984; 48: 1127–1134.
33. Holland T J B, Powell R. An improved and extended internally consistent thermodynamic dataset for phases of petrological interest, involving a new equation of state for solids. *J Metamorph Geol.* 2011; 29: 333–383.
34. Huang S J. Carbonate diagenesis. Geological Press. 2010. pp. 73.
35. Soli A L, Byrne R H. CO₂ system hydration and dehydration kinetics and the equilibrium CO₂/H₂CO₃ ratio in aqueous NaCl solution. *Mar Chem.* 2002; 78: 65–73.
36. Zhang Z J. Discussion on the several questions of the determination of carbonic acid in natural water. *Journal of Yangling Vocational & Technical College.* 2007; 6: 9–11 (in Chinese with English Abstract).
37. Bhirud V L. A four-parameter corresponding states theory: saturated liquid densities of anormal fluids. *Aiche J.* 1978; 24: 880–885.
38. Sverjensky D A, Shock E L, Helgeson H C. Prediction of the thermodynamic properties of aqueous metal complexes to 1000°C and 5 kb. *Geochim Cosmochim Ac.* 1997; 61: 1359–1412.
39. Xu J, Fan C F, Teng H H. Calcite dissolution kinetics in view of Gibbs free energy, dislocation density, and P_{CO2}. *Chem Geol.* 2012; 322–323: 11–18.
40. Mandalaparty P. Reaction chemistry in carbon dioxide sequestration. UMI dissertation publishing: The University of Utah. 2012.
41. Lundegard P D, Land L S. Carbonate equilibria and pH buffering by organic acids—response to changes in P_{CO2}. *Chem Geol.* 1989; 74: 277–287.
42. Bateman K, Turner G, Pearce J M, Noy D J, Birchall D, Rochelle C A. Large-Scale Column Experiment: Study of CO₂, Porewater, Rock Reactions and Model Test Case. *Oil & Gas Sci. Technol.—Rev. IFP.* 2005; 60: 161–175.
43. Guimaraes L, Abreu H A, Duarte H A. Fe(II) hydrolysis in aqueous solution: A DFT study. *Chem Phys.* 2007; 333: 10–17.

44. Chai L, Navrotsky A Synthesis, characterization, and energetics of solid solution along the dolomite-ankerite join, and implications for the stability of ordered $\text{CaFe}(\text{CO}_3)_2$. *Am Mineral*. 1996; 81: 1141–1147.